A Phase-Locked Loop Continuous Wave Sonic Anemometer-Thermometer[1]

S. E. LARSEN,[2] F. W. WELLER AND J. A. BUSINGER

Department of Atmospheric Sciences, University of Washington, Seattle 98195

(Manuscript received 23 September 1977, in final form 10 November 1978)

ABSTRACT

A continuous wave sonic anemometer-thermometer has been developed for simultaneous measurements of vertical velocity and temperature. The phase angle fluctuations are detected by means of a monolithic integrated phase-locked loop, the latter feature providing for inexpensive and accurate electronics. The principle is described and discussed.

1. Introduction

Because of a number of attractive characteristics (linear, fast response and lack of moving parts) sonic anemometers have become widely used instruments in the study of atmospheric turbulence within the last decade.

So far, essentially two different ways of operation have been utilized: The pulsed type sonic anemometer determines the velocity and temperature fluctuations by measuring the difference and the sum of transit times for two series of sound pulses travelling in opposite directions along a given path (Barrett and Suomi, 1949). The continuous wave sonic anemometer is based on the same general principle, but, instead of pulses, continuous signals of two different frequencies are used for transmission in the two directions (the frequencies are different to avoid cross-talk between the channels). The information about transit times is obtained by detecting the phase differences across the path (Kaimal and Businger, 1963). Also a hybrid instrument has been developed which uses pulses consisting of wave packets (Mitsuta *et al.*, 1967).

The instrument described here is of the continuous wave type with the modification that a phase-locked loop is used to keep the phase differences across the sound path constant, irrespective of wind- and sound-velocity variations, by varying the frequency of the sound waves. Hence information about the transit times is given in terms of frequency variation of the sound waves.

2. Principles of operation

In Fig. 1 the principle of operation for one sound path is outlined.

The time it takes for a given phase plane in the sound wave to cross the gap between the transmitter and the receiver is given by

$$\Delta t = \frac{d}{c\cos\alpha + w}, \quad (1)$$

where the wind velocity has been decomposed in a component w along the line TR and a component in the plane perpendicular to this line, V_h, where $\sin\alpha = V_h/c$, where c is the speed of sound.

The phase difference between R and T for a wave

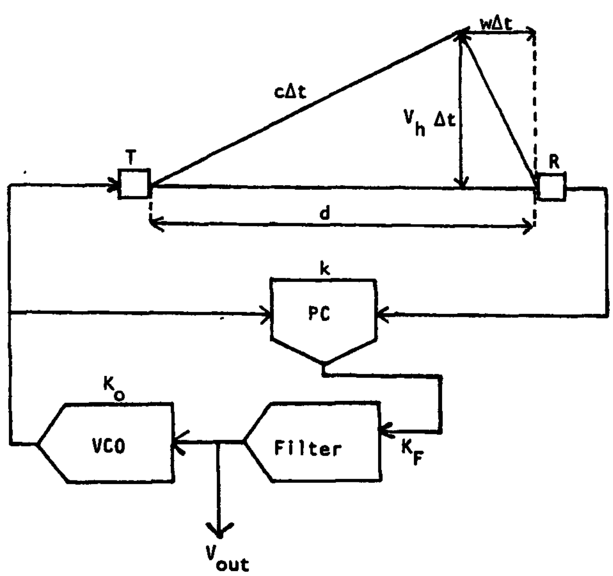

FIG. 1. Operating principle for one sonic channel. T is the transmitter and R is the receiver. PC is the phase comparator and VCO is the voltage regulated oscillator. k is the transfer coefficient of the phase comparator (V rad^{-1}) and k_0 the transfer coefficient of the voltage regulated oscillator (rad s^{-1} V^{-1}), while k_F is the dc gain of the low-pass filter.

[1] Contribution No. 455, Department of Atmospheric Sciences, University of Washington.

[2] On leave from Risø National Laboratory, Roskilde, Denmark.

0021-8952/79/040562-07$05.75

train of frequency ω is given by

$$\psi=\omega\Delta t=\frac{\omega d}{c\cos\alpha+w}. \quad (2)$$

The output of the phase comparator will be zero for a given phase difference ψ_0 (in this case $\frac{1}{2}\pi+n\pi$). If the actual phase difference ψ is different from ψ_0 the phase comparator will give a voltage input to the voltage-regulated oscillator, thereby changing its frequency so that $\psi\rightarrow\psi_0$. If $\psi=\psi_0$, the oscillator will receive zero input and will oscillate at its free running frequency ω_0. By setting ω_0 in zero wind conditions one obtains

$$\psi_0=\omega_0\Delta t_0=\frac{\omega_0 d}{c_0}, \quad (3)$$

where c_0 is the speed of sound under the conditions where ω_0 is determined.

First we shall illustrate the operation of the instrument by assuming a perfect phase lock, i.e., that $\psi=\psi_0$ for all Δt. Equating (2) and (3) we obtain

$$\frac{\omega-\omega_0}{\omega_0}=\frac{w}{c_0}+\frac{c}{c_0}\cos\alpha-1. \quad (4)$$

Correspondingly an opposite transmission direction yields

$$\frac{\omega_1-\omega_{01}}{\omega_{01}}=-\frac{w}{c_0}+\frac{c}{c_0}\cos\alpha-1. \quad (5)$$

Summing and differencing those two equations we can write

$$\frac{\omega-\omega_0}{\omega_0}+\frac{\omega_1-\omega_{01}}{\omega_{01}}=2\left(\frac{c}{c_0}\cos\alpha-1\right), \quad (6)$$

$$\frac{\omega-\omega_0}{\omega_0}-\frac{\omega_1-\omega_{01}}{\omega_{01}}=2\frac{w}{c_0}. \quad (7)$$

We will compare these equations with the equations for two other methods used for reducing data from sonic anemometers. The first is most commonly used and can be written (Kaimal and Businger, 1963)

$$\Delta t+\Delta t_1=\frac{2dc\cos\alpha}{c^2-V_h^2-w^2}, \quad (8)$$

$$\Delta t-\Delta t_1=\frac{2dw}{c^2-V_h^2-w^2}. \quad (9)$$

The second method, although known for some time, has not been applied in practice as far as we know. It consists of adding and subtracting the reciprocal travel times, i.e.,

$$\Delta t^{-1}+\Delta t_1^{-1}=2c\cos(\alpha/d), \quad (10)$$

$$\Delta t^{-1}-\Delta t_1^{-1}=2w/d. \quad (11)$$

Comparison of these sets of equations lead to the following conclusions:

1) The phase-locked loop method has the advantages that the path length d drops out and that only measurements of relative frequency variations are necessary.

2) In the phase-locked loop method and in the second method mentioned above, w measurements are not contaminated with variations in c and V_h, as they are in the first method (see Friehe, 1976).

3) All methods share the disadvantage that measurements of c, and thereby of the virtual temperature deduced from c (see Kaimal and Businger, 1963) are contaminated with velocity fluctuations (Friehe, 1976).

3. Static response of the instrument

In this section it will be shown how (4) is realized in the actual instrument for static conditions, i.e., a constant $\Delta t\neq\Delta t_0$ and furthermore what the constraints on d are, although this quantity does not appear in the ideal response equations (6) and (7). For simplicity phase distortion in transducers is neglected in this section and treated separately in the next section.

When the phase is locked in the system the output of the phase comparator can be written (Viberti, 1966)

$$V_{\mathrm{out}}=KK_F(\psi_0-\psi), \quad (12)$$

where K is the transfer coefficient of the phase comparator (V rad^{-1}) and K_F is the dc gain of the filter. ψ_0 and ψ are given by (3) and (2). For static consideration we can neglect the filter characteristic of the filter following the comparator.

The frequency of the oscillator is related to V_{out} through

$$\omega-\omega_0=K_0V_{\mathrm{out}}\equiv\frac{\omega_0}{k_0}V_{\mathrm{out}}, \quad (13)$$

where K_0 is the transfer coefficient of the voltage-regulated oscillator (rad s^{-1} V^{-1}), the proportionality between K_0 and ω_0, and where the constant of proportionality k_0^{-1} is insured by the fact that ω_0 and K_0 are determined by the same resistance capacitance product. Combination of (10) and (11) yields

$$V_{\mathrm{out}}=k_0\frac{(\omega-\omega_0)}{\omega_0}=k_0\frac{\Delta t_0-\Delta t}{\Delta t}[1+(K_0KK_F\Delta t)^{-1}]^{-1}. \quad (14)$$

If we substitute (1) and (3) and denote K_0KK_F by K_L, which is called the loop gain, we can write (14) as

$$V_{\mathrm{out}}=k_0\left[\frac{w}{c_0}+\left(\frac{c}{c_0}\cos\alpha-1\right)\right]\left[1+\frac{c\cos\alpha+w}{K_Ld}\right]^{-1}. \quad (15)$$

By comparison with (4), it is seen that the conditions for ideal response is that

$$\frac{K_Ld}{c}\gg1.$$

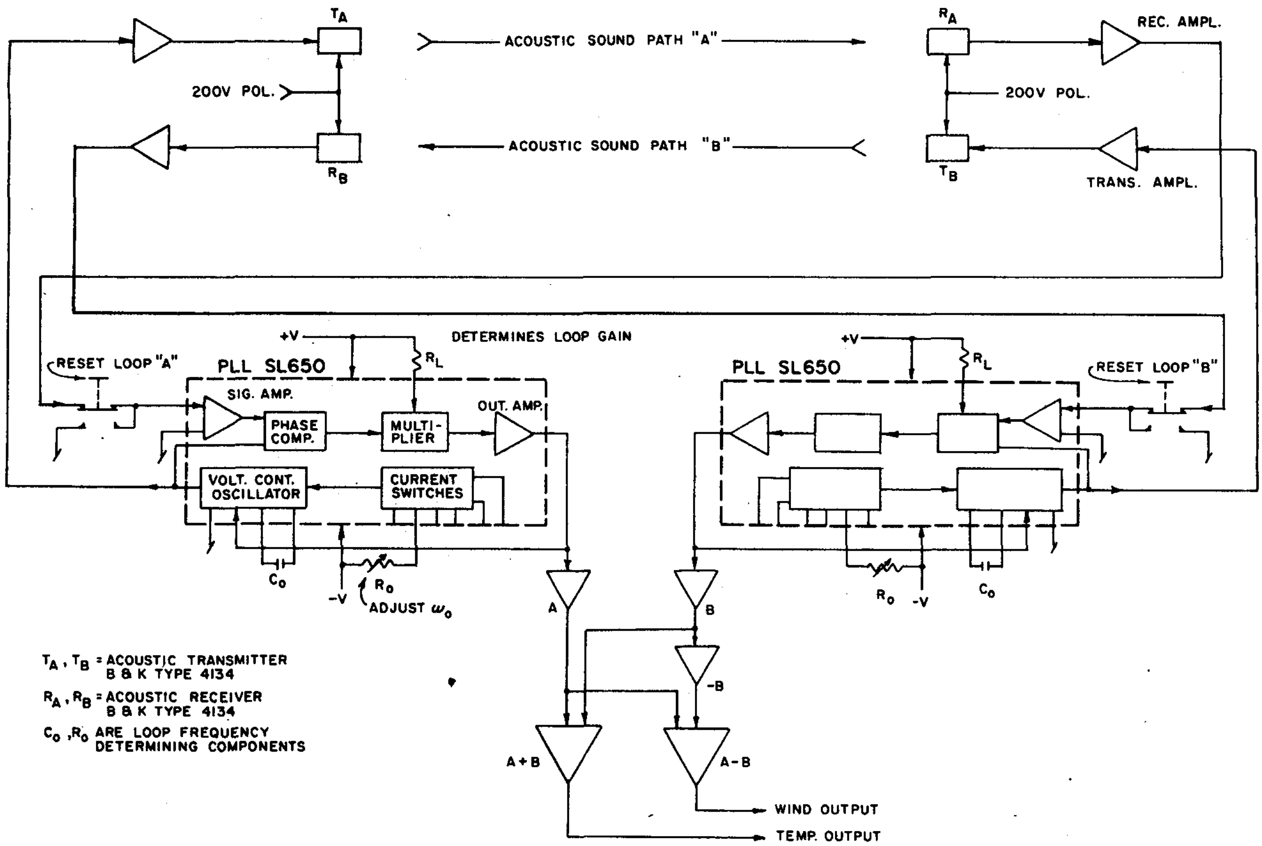

FIG. 2. Block diagram of the phase-locked loop (PLL) sonic anemometer for measuring one velocity component and virtual temperature. The transducers are Brüel and Kjaer condenser microphones having a diameter of $\frac{1}{4}$ inch. The preamplifiers are also B & K amplifiers matched to the transducers.

Assuming $K_L d > 10c$ and V_h and w less than $c/10$, the correction factor in (15) becomes a second-order term, i.e.,

$$\left(1+\frac{c\cos\alpha+w}{K_L d}\right)^{-1}\approx 1-\frac{c}{K_L d}\left(1-\frac{c}{K_L d}\right)-\frac{w}{K_L d}. \quad (16)$$

For the instrument now in use K_L is about 3×10^5 s^{-1} and d about 10 cm, yielding a correction of the order of 1%. Since the main correction term is proportional to c it varies very little and can therefore easily be taken into account by a calibration. Another constraint may be formulated by subtracting (3) from (2), which yields

$$\Delta\psi=\psi-\psi_0=\frac{\omega d}{c\cos\alpha+w}-\frac{\omega_0 d}{c_0}.$$

We may now ask how much w has to change before an ambiguity in the response is generated, i.e., $|\Delta\psi|\geqslant\pi$. Starting with $w=0$ and $c=c_0$ and neglecting $\cos\alpha$, we find

$$\left|\frac{\Delta w}{c}\right|>\frac{\pi c_0}{\omega_0 d-\pi c_0}\approx\frac{\pi c_0}{\omega_0 d}\approx\frac{c_0}{2f_0 d},$$

where f_0 is the frequency (Hz). If we let $f_0=20$ kHz and $d\approx10$ cm,

$$|\Delta w|\geqslant 28.9 \text{ m s}^{-1}$$

which is an enormous velocity change and which for smaller d becomes even larger. This constraint presents no problem for most applications.

If, however, we consider the noise $\Delta\psi_n$ in the phase comparator reduced to input, we have another constraint given by the minimum resolvable velocity change. Again from (2) and (3) we may derive

$$\frac{w_{\min}}{c_0}\approx\frac{\Delta\psi_n c_0}{\omega_0 d}.$$

For a given $\omega_0 d$ this indicates that we should maximize $\omega_0 d$. The noise level in the system is low enough that with $d\approx10$ cm we can resolve fluctuations in $w<1$ cm s^{-1}.

We conclude, therefore, that d is primarily determined by the physical constraint of the size of the transducers and the desire to measure the smallest possible eddies.

From V_{out} in (15) and the corresponding V_{out} for the opposite transmission direction, estimates of w and $c(T,e)$ are obtained by simple adding and differencing circuits, as shown in Fig. 2.

4. Phase lag in transducers

The equations in Sections 2 and 3 presuppose that the transducers have an ideal flat phase response. Based on the principles of an ideal phase lock, as in Section 2, the present section discusses the influence of phase lag in the transducers.

We let $\phi(\omega)$ describe the total phase lag in the transmitter and the receiver. Corresponding to (2) and (3) the phase difference between input and output of the phase comparator can be written

$$\left.\begin{aligned}\psi_r&=\psi+\phi(\omega)\\ \psi_{r0}&=\psi_0+\phi(\omega_0)\end{aligned}\right\}, \qquad (17)$$

where ψ and ψ_0 are given by (2) and (3), respectively.

After substituting (2) and (3) in (17) and letting $\psi_r=\psi_{r0}$, we obtain the following equation, corresponding to (4):

$$\frac{\omega-\omega_0}{\omega_0}=\frac{w}{c_0}+\frac{c}{c_0}\cos\alpha-1+\frac{(c\cos\alpha+w)}{\omega_0 d}[\phi(\omega_0)-\phi(\omega)]. \qquad (18)$$

We now assume that the phase lag varies linearly with frequency in the frequency interval considered, i.e.,

$$\phi(\omega_0)-\phi(\omega)=k(\omega_0-\omega). \qquad (19)$$

Eq. (18) then becomes

$$\frac{\omega-\omega_0}{\omega_0}=\left(\frac{w}{c_0}+\frac{c}{c_0}\cos\alpha-1\right)\left(1+\frac{c\cos\alpha+w}{d}k\right)^{-1}. \qquad (20)$$

As in (15) and (16) the leading term in the correction factor is here seen to be ck/d and the conditions for ideal response is that this quantity is much smaller than 1.

For our transducers we find from the manufacturers information that in the frequency interval 20–40 KHz one can use $k\approx 3\times 10^{-6}$ s^{-1}, which with $d=10$ cm, yields a correction factor of 1% in (20). As in (15) we therefore have a correction factor of the order of 1%, which since it is proportional to c varies very little with environmental conditions. The factor k on the other hand must be expected to be somewhat uncertain, however, both because the description of the phase lag in (19) can be considered an approximation only and because differences between individual transducers must be expected. We therefore conclude that the best method for taking into account this correction factor is a wind tunnel calibration.

5. Dynamic response

Considered as a dynamic system the instrument, even when phase-lock is achieved, is controlled by a highly nonlinear equation, which evades a simple analysis. An approximate linear description, however, can be obtained by the following arguments.

The response to a time varying delay time $\Delta t(t)$ can be approximated by comparing (12) and (13) from which we obtain

$$\omega(t)-\omega_0=K_L\int_{-\infty}^{\infty}F(t-\tau)[\omega_0\Delta t_0-\omega(\tau)\Delta t(\tau)]d\tau, \qquad (21)$$

where $F(t)$ is the unit pulse response function of the filter (see Fig. 1).

Since the variation of $\Delta t(t)$ is due to variation in the wind and sound velocity we can write from (1)

$$\Delta t(t)=\frac{d}{n(t)}=\frac{d}{n_s+n'(t)}\approx\frac{d}{n_s}\left(1-\frac{n'(t)}{n_s}\right), \qquad (22)$$

where $n(t)$ has a fluctuating component $n'(t)$ and a static component $n_s\gg n'$. Correspondingly we can write $\omega(t)=\omega_s+\omega'(t)$. Substituting these definitions into (21) we obtain (neglecting the second-order term $\omega'n'$)

$$\omega'(t)=K_L\int_{-\infty}^{\infty}F(t-\tau)\left[-\frac{d}{n_s}\omega'(\tau)+\frac{\omega_s d}{n_s^2}n'(\tau)\right]d\tau, \qquad (23)$$

whose Fourier transform is

$$\frac{\hat{\omega}'(\Omega)}{\omega_s}=\frac{K_L\hat{F}(\Omega)}{n_s/d+K_L\hat{F}(\Omega)}\frac{\hat{n}'(\Omega)}{n_s}, \qquad (24)$$

where $\hat{\omega}'(\Omega)$, $\hat{F}(\Omega)$ and $\hat{n}'(\Omega)$ are the Fourier transforms of $\omega'(t)$, $F(t)$ and $n'(t)$. By use of (14), with $K_L d/c\gg 1$, we can write (20) as

$$\hat{V}_{\rm out}(\Omega)=\frac{k_0K_L\hat{F}(\Omega)}{n_s/d+K_L\hat{F}(\Omega)}\left[\frac{\hat{w}(\Omega)}{c_0}+\widehat{\left(\frac{c}{c_0}\cos\alpha-1\right)}(\Omega)\right]. \qquad (25)$$

The filter used in the loop is of the low-pass type and is introduced in the loop to optimize the loop behavior (Viberti, 1966) and to damp out a strong component of the phase comparator output at twice the oscillator frequency. It starts attenuating at 400 Hz. From (25) it is seen that as long as $K_L|\hat{F}(\Omega)|d/n_s\gg 1$ there is no attenuation of the fluctuating components by the loop. For frequencies where $\hat{F}(\Omega)$ does not attenuate this criterion corresponds to the criterion for neglecting the correction term in (15), which was seen to be justified for the present design.

6. Discussion

The array and the control unit of the prototype instrument built at the University of Washington are displayed in Fig. 3. The two sound paths shown operate at free running frequencies of 19 and 39 kHz. From (4) we see that measurements of velocities up to 35 m s^{-1} need about 10% frequency range corresponding to 1.9 and 3.9 kHz respectively, in which frequency interval the phase transfer of the transducers must be rather

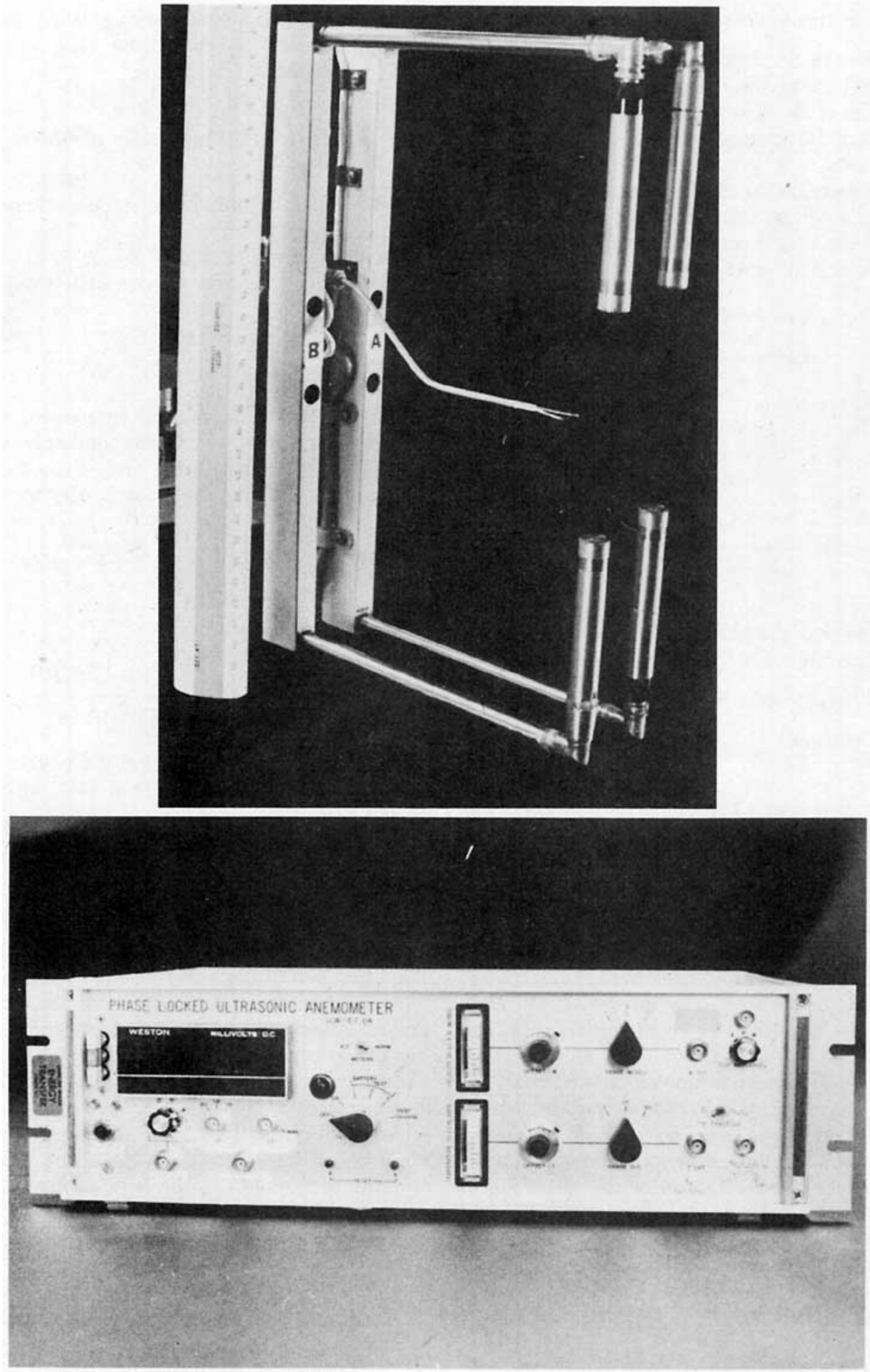

FIG. 3. Photograph of phase-locked loop sonic anemometer array and control panel.

flat, as shown in Section 4. So far the only transducers fulfilling this requirement, we have found, have been condenser microphones. These transducers, however, have a number of drawbacks, such as the need for a high (200 V) bias voltage and special preamplifiers which must be placed close to the transducers, and which increase the size of the array. Also these transducers are expensive and not very weatherproof. The present instrument not including design and engineering time costs about $2500 of which the transducers alone cost $1900. It is therefore our hope that soon a piezoceramic microphone with the desired phase characteristics will be developed. This would reduce the price and eliminate the need for a high voltage bias.

The bottom part of Fig. 3 shows the front panel of the control unit. There are three ranges for w and T (1, 3 and 10 m s^{-1}, and 1, 10 and 30°C, respectively). The digital voltmeter on the left of the front panel can be used to monitor voltages from loop A and B (see Fig. 2), or w or T. The temperature is measured also with a $\frac{1}{2}$ mil diameter type E thermocouple which is mounted in the center of the array as can be seen in the upper part of Fig. 3.

A disadvantage of the instrument is its rather high zero drift, this drift being mainly due to drift in ω_0 which at best is of the order of 20 ppm °C^{-1} for the SL650 phase locked loop circuit. Through Eq. (4) this is seen to correspond to an apparent velocity drift given by

$$w_{\mathrm{drift}} \approx 2\times 10^{-5} c \approx 0.7 \text{ cm s}^{-1}\ {}^{\circ}\mathrm{C}^{-1}. \qquad (26)$$

This drift can be corrected for by monitoring ω_0 on the frequency counters. For the SL650 the lock and capture ranges are defined by $1/C_0R_L$, where the capacitance C_0 and the resistor R_L are shown on Fig. 2. Since R_L is made large, the loop tends to become unlocked in wind gusts $\geqslant 10$ m s^{-1}. To restore phase lock we have incorporated on the front panel two manual loop reset buttons, visible under the on-off switch (Fig. 3) bottom.

For adjusting ω_0 on A and B an averager with a time constant of 100 s is built into the instrument. Bandpass

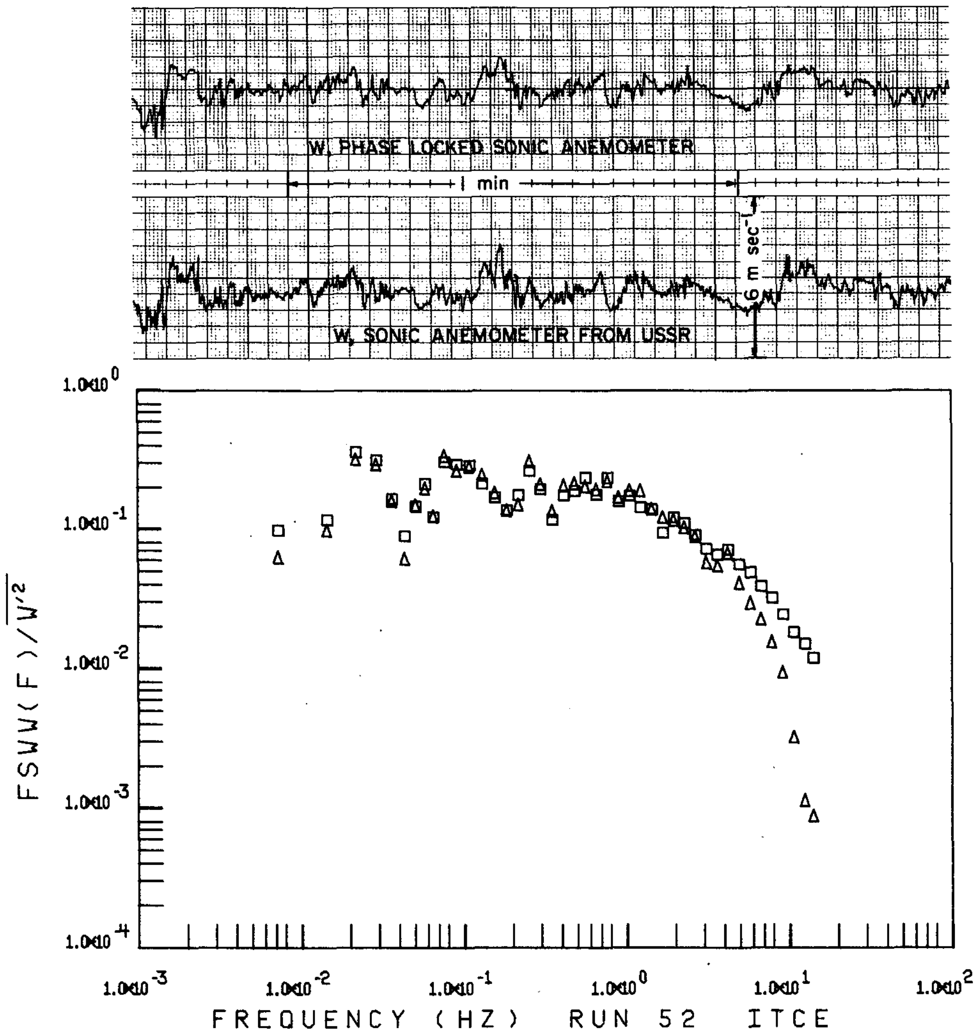

FIG. 4. Comparison of vertical velocity signals of the PLL sonic with the sonic anemometer from USSR during the ITCE experiment in Australia 1976. The effect of a 6 Hz filter on the PLL sonic can be seen in the smoothing of the high-frequency information in the PLL sonic anemometer spectrum (△). The USSR sonic anemometer spectrum (□) shows only the roll-off introduced by line averaging along the acoustic path.

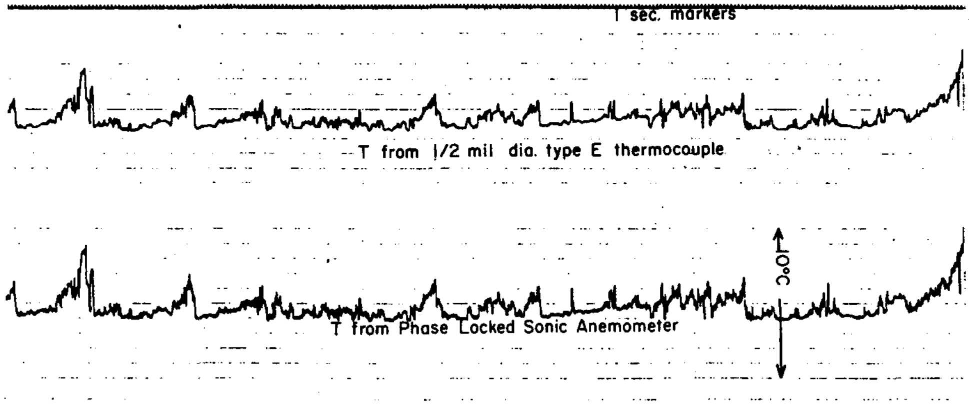

FIG. 5. Comparison of T from PLL anemometer and 12.5 μm diameter thermocouple mounted in center of array.

filters with a frequency band of 0.0001 to 10 Hz are built into the instrument for analog computation of heat flux. w' and T' are also available on front panel connectors.

In the present instrument the noise level for the w output is <0.5 cm s^{-1} and for the T output ~ 0.01°C. Frequency response of the phase locked loop is 400 Hz. The frequency response of the w measurement is limited by the line averaging along d which, in turn, is determined by the transducer size.

Some results obtained with the instrument during the International Turbulence Comparison Experiment (ITCE) which was held in Australia (fall 1976) are given in Figs. 4 and 5. Fig. 4 shows the traces of w obtained with the USSR sonic anemometer, which is used by the Institute of Atmospheric Physics in Moscow, and the corresponding spectra. The agreement is good except for the high-frequency end of the spectrum. The signal from the PLL sonic anemometer was filtered with a 6 Hz low-pass filter which accounts for the early roll-off of the PLL data. The two instruments were mounted on the same mast and their horizontal separation was about 0.5 m. Fig. 5 shows the temperature obtained with the $\frac{1}{2}$ mil thermocouple mounted in the center of the array and the temperature obtained with the PLL sonic anemometer-thermometer. The agreement is excellent in detail.

Acknowledgments. This work was supported by the Atmospheric Research Section of the National Science Foundation under Grants ATM 76-00855 A01 and ATM 77-23715. Special thanks are due to Dr. J. Chandan Kaimal for his comments and critical review of the paper and to William Shaw for the ITCE data he provided.

REFERENCES

Barrett, E. W., and V. E. Suomi, 1949: Preliminary report on temperature measurement by sonic means. *J. Meteor.*, **6**, 273–276.

Friehe, C. A., 1976: Effects of sound speed fluctuations on sonic anemometer measurements. *J. Appl. Meteor.*, **15**, 607–610.

Kaimal, J. C., and J. A. Businger, 1963: A continuous wave sonic anemometer-thermometer. *J. Appl. Meteor.*, **2**, 156–164.

Mitsuta, Y., M. Miyake and Y. Kobori, 1967: Three-dimensional sonic anemometer-thermometer for atmospheric turbulence measurements. *Disast. Prev. Res. Inst. Kyoto Univ.*, WDD Tech. Note, Japan.

Viterbi, A. J., 1966: *Principles of Coherent Communication*. McGraw Hill, 321 p.